

High-pressure x-ray diffraction studies of the nanostructured transparent vitroceraic medium $K_2O-SiO_2-Ga_2O_3$

K. E. Lipinska-Kalita,^{1,*} B. Chen,^{1,†} M. B. Kruger,¹ Y. Ohki,² J. Murowchick,³ and E. P. Gogol⁴

¹*Department of Physics, University of Missouri—Kansas City, Kansas City, Missouri 64110, USA*

²*Department of Electrical, Electronics, and Computer Engineering, Waseda University, 3-4-1 Ohkubo, Shinjuku-ku, Tokyo 169-8555, Japan*

³*Department of Geosciences, University of Missouri—Kansas City, Kansas City, Missouri 64110, USA*

⁴*School of Biological Sciences, University of Missouri—Kansas City, Kansas City, Missouri 64110, USA*

(Received 21 January 2003; published 17 July 2003)

Synchrotron-radiation-based, energy-dispersive x-ray-diffraction studies have been performed on a composite containing nanometer-size aggregates embedded in an amorphous matrix, in the pressure range from ambient up to 15 GPa. The optically transparent material containing β - Ga_2O_3 nanocrystals was developed by the controlled crystallization of a silicon oxide-based amorphous precursor. Transmission electron microscopy and conventional x-ray-diffraction techniques allowed estimating the mean size of a single-crystalline phase to be 14.8 ± 1.9 nm, distributed homogeneously in an amorphous medium. The pressure-driven evolution of x-ray-diffraction patterns indicated a progressive densification of the nanocrystalline phase. A structural modification corresponding to a pressure-induced coordination change of the gallium atoms was evidenced by the appearance of new diffraction peaks. The overall changes of x-ray-diffraction patterns indicated a β - Ga_2O_3 to α - Ga_2O_3 phase transformation. The low- to high-density phase transition was initiated at around 6 GPa and not completed in the pressure range investigated. A Birch-Murnaghan fit of the unit-cell volume change as a function of pressure yielded a zero-pressure bulk modulus, K_0 , for the nanocrystalline phase of 191 ± 4.9 GPa and its pressure derivative, $K_0' = 8.3 \pm 0.9$.

DOI: 10.1103/PhysRevB.68.035209

PACS number(s): 61.46.+w, 61.10.Nz, 62.50.+p, 64.30.+t

I. INTRODUCTION

Composites containing nanometer-size structures of metal, semiconductor, or dielectric clusters in solid matrices are currently attracting much consideration because of their diverse technological applications. Among these materials, optically transparent glass ceramics have been extensively investigated because of their function as promising nonlinear media for optical processing devices.¹⁻⁷ High-pressure studies of nanostructured analogs of bulk materials, that is, of nanosized structures, are critical for identifying equilibrium and metastable states, that can be accessed as these materials are compressed to very small volumes. Pressure-driven modifications of such structures are attractive from both a fundamental physics point of view as well as the exciting prospect of fabricating different materials. Most high-pressure research on nanocrystalline materials has been done on granular media (powders) with the average grain size of nanometer dimensions. Nevertheless, the kinetics of pressure-driven structural transformations between different nanosized phases is poorly understood. It appears to be obvious that in the case of phase transitions occurring in the nanocrystals embedded in solid matrices, the representation is more complex, in particular, when the host matrix network-forming units may also undergo pressure-stimulated structural transformation. This matter is among the most fascinating unsolved problems and it is the point of interest of our research.

The composite material synthesized for high-pressure investigations in this study is made of silicon oxide-based host glass homogeneously doped by nanocrystalline gallium ox-

ide. The host glass network is built of a three-dimensional structure composed of corner-shared tetrahedra, and it was demonstrated to undergo structural transformations when subjected to high pressure.⁸⁻¹⁷ The gallium ions were selected as dopants for our system since in the controlled nucleation process they form nanocrystals with a well-defined structure of β - Ga_2O_3 homogeneously dispersed in the host glass matrix.^{1,18} Moreover, bulk β - Ga_2O_3 is one of the widest band-gap oxides and recently attracted much research interest due to its prospective applications as a transparent conducting oxide in optoelectronics.¹⁹⁻²² In ambient conditions the thermodynamically stable form of gallium oxide is β - Ga_2O_3 , which has a monoclinic unit cell and belongs to the space group $C2/m$. However, the compound shows polymorphism and according to the literature, depending on temperature-pressure-atmosphere conditions, can appear in five different (α , β , γ , σ , ϵ) stable or metastable crystal structures.^{23,24}

The present study had two goals. The first was to synthesize oxide glass-based optically transparent vitroceraic media, with a single-crystalline phase of controlled-size nanocrystals homogeneously dispersed throughout the composite; the second was to study pressure-induced structural transformations in the nanocrystalline phase of these materials, in which the metastability of the host matrix is relieved by nucleation and growth processes. Using a synchrotron-radiation-based x-ray-diffraction technique and diamond-anvil cells we followed *in situ* the pressure-induced changes in the structure of β - Ga_2O_3 nanocrystals embedded in a glass-based composite material. The structural transformation occurring in the nanocrystalline phase was studied in the

pressure range for which the literature already reports structural rearrangements corresponding to the beginning of the tetrahedral to octahedral coordination change and pressure-induced densification of the tetrahedral glass networks.^{8,9,11–15,17} To the best of our knowledge, this work is the first attempt to measure the equation of state of nanocrystals embedded in an optically transparent amorphous tetrahedral framework.

II. EXPERIMENT

A mixture for the potassium silicate precursor glass doped by gallium ions, of nominal composition represented by a 4 K: 8 Ga: 24 Si: 64 O ratio in at. %, was prepared using analytical grade reagents of 99.999% purity. The batch components were sintered at low temperature and afterwards melted in a platinum crucible at a temperature varying between 1550 °C and 1600 °C in a resistance furnace in an air atmosphere. The liquid melt was cast into a brass mold and air cooled. To induce partial crystallization, rectangular pieces of material underwent gradual isothermal heat treatments. This treatment allowed us to obtain composites with different diameters of the nanocrystalline phase.

In order to perform the structural characterization of the synthesized materials, high-resolution transmission electron microscopy (HRTEM) and two x-ray-diffraction techniques were applied: conventional angle- and energy-dispersive synchrotron-radiation-based x-ray diffraction. To confirm the amorphous structure of the as-quenched glass and to identify the structure of the nanocrystalline phase, conventional x-ray-diffraction (XRD) spectra were collected on a Rigaku Miniflex diffractometer (36 KV/15 mW) with a variable slit, in θ - 2θ Bragg-Brentano geometry, using Cu K_α radiation and a scintillation detector in the 2θ range between 20° and 80°. The particle size was estimated from the broadening of Bragg peaks using the Scherrer formula²⁵ as well as from the HRTEM micrographs.

For high-pressure studies, a sample with a mean size of the nanocrystalline phase of 14.8 ± 1.9 nm was selected. The energy-dispersive x-ray-diffraction spectra were measured at beam line X17C of the National Synchrotron Light Source at Brookhaven National Laboratory. The beam was focused to $10 \times 10 \mu\text{m}$ square and a liquid-nitrogen-cooled Ge detector was used. The sample was compressed in a Mao-Bell-type diamond-anvil cell (DAC) with diamonds having 350- μm culet diameters. The sample chamber consisted of a 150- μm hole drilled in a preindented spring-steel gasket. The sample, with a diameter of 30 μm , along with a few grains of gold for determining pressure²⁶ and a 4:1 methanol-ethanol mixture as a pressure-transmitting medium, was loaded in the chamber. The diffraction spectra were measured in the DAC, at pressures from ambient up to 15 GPa. All data were collected at 295 K with a scattering angle $2\theta = 10.005 \pm 0.003^\circ$. The estimated pressure variation over the x-rayed sample was less than ± 0.25 GPa. High-resolution transmission electron micrographs of the powdered samples spread over carbon-coated copper grids were obtained by using a JEOL EX II microscope, operating at 120 kV.

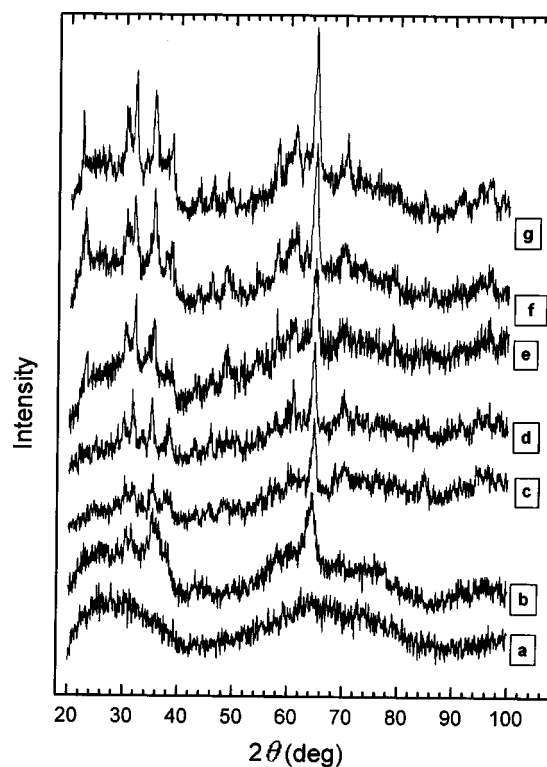


FIG. 1. (a) Conventional, angle-dispersive x-ray-diffraction patterns for the as-quenched glass and (b)–(g) for samples annealed between 600 °C and 1100 °C, indicating a progressive crystallization of monoclinic gallium oxide. The estimated mean particle size changes from 6.5 ± 0.8 to 25.5 ± 2.5 nm.

III. RESULTS

Both XRD and HRTEM confirmed the amorphous nature of the as-quenched glass. A distinct change in the microstructure occurred after thermal annealing and crystallization of the monoclinic β - Ga_2O_3 phase was observed, with grain size increasing with annealing temperature and time. The angle-dispersive XRD spectra of as-quenched glass and of the samples annealed at different temperatures are presented in Fig. 1. The diffraction spectrum of the as-quenched glass exhibits two broad bands in the 2θ range, 20°–100°, typical of glass systems. The crystallite size in the annealed samples was calculated applying the Scherrer equation that relates the broadening of an x-ray beam to the crystal size.²⁶ The crystallite size and distribution were also evaluated using HRTEM. The mean diameter of the nanocrystalline phase increased from 6.5 ± 0.8 to 25.5 ± 2.5 nm for the samples annealed at various temperatures (Fig. 1). The average diameter of nanocrystalline phase estimated from HRTEM was in agreement with the calculations based on XRD patterns and the Scherrer equation. Figure 2(a) is a HRTEM micrograph showing the microstructure of the as-quenched glass. Selected area electron-diffraction (SAD) patterns did not reveal any crystalline reflection but only presented the halo typical of amorphous systems. Figure 2(b) shows the micrograph of one of the annealed samples, where the coherently scattering domains are uniformly distributed inside the amorphous matrix indicating the nucleation of nanocrystals. The estimated

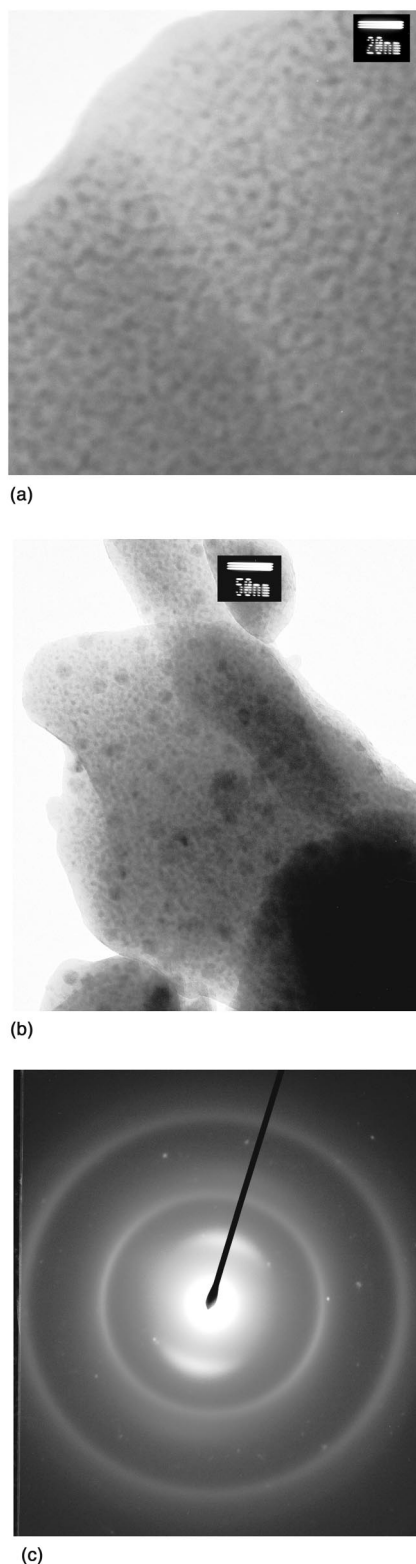


FIG. 2. TEM micrographs indicating the change in the microstructure from amorphous to polycrystalline: (a) as-quenched glass, (b) annealed sample showing gallium oxide nanocrystals with a mean diameter of 14.8 ± 1.9 nm, and (c) selected area diffraction pattern of the annealed sample with very fine diffraction rings due to β - Ga_2O_3 nanocrystals of 14.8 ± 1.9 nm diameter.

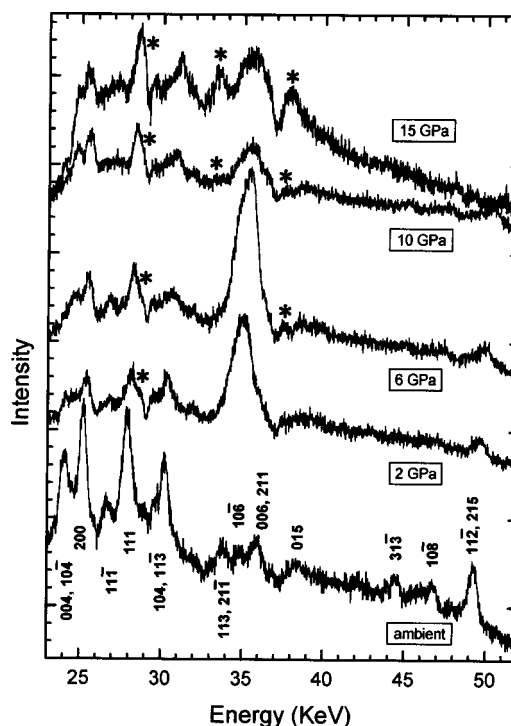


FIG. 3. Synchrotron-radiation-based, energy-dispersive x-ray-diffraction spectra collected in the pressure range from ambient up to 15 GPa. The data were collected at ambient temperature and in hydrostatic conditions up to around 10 GPa. Stars denote Bragg peaks assigned to the alpha phase of gallium oxide as discussed in the text.

crystallite size was 15.9 ± 0.8 nm. An amorphous structure is still present in this sample, as confirmed by XRD and by the diffuse halo visible in the SAD patterns [Fig. 2(c)]. The very fine rings visible in the SAD patterns for the annealed samples confirm the presence of a crystalline phase [Fig. 2(c)].

For the high-pressure investigations we selected a glass-ceramic composite with gallium oxide nanoparticles of mean diameter of 14.8 ± 1.9 nm (15.9 ± 0.8 nm as found from HR-TEM and 14.5 ± 1.6 nm as calculated using the Scherrer equation) homogeneously distributed in an optically transparent amorphous matrix. Figure 3 shows the synchrotron-radiation-based energy-dispersive x-ray-diffraction patterns of the nanocrystalline glass-ceramic composite in the pressure range from ambient up to 15 GPa. At ambient and low pressures, all of the observed Bragg peaks agree well with the reference data of β - Ga_2O_3 (JCPDS International Center for Diffraction Data card number 11-370). However, an increase in pressure introduces a few new peaks that were attributed to the new phase corresponding to α - Ga_2O_3 .

The observed and calculated interplanar d_{hkl} spacings of the β - Ga_2O_3 phase are presented in Table I, and the variations of the lattice-plane spacings as a function of pressure are shown in Figs. 4(a) and 4(b). A nonlinear, multivariate least-squares-fitting procedure was used to determine the unit-cell parameters of the crystal structure (a , b , c , and θ) from the d spacings and our zero-pressure measurements are in good agreement with previously reported results (Fig. 5).²³

TABLE I. Interplanar $d_{h,k,l}$ spacing for the β -Ga₂O₃ phase derived from the ambient pressure, synchrotron-radiation-based diffraction data (for strong Bragg peaks only) and the values calculated assuming the monoclinic crystal lattice. The unit-cell parameters derived from the experimental data are compared with those of Geller (Ref. 23) for β -Ga₂O₃.

Nanophase β Ga ₂ O ₃			
Intensity	d_{exp} (Å)	d_{cal} (Å)	$h k l$
100	2.954	2.959	004
100	2.819	2.823	200
70	2.671	2.676	11-1
100	2.548	2.549	111
80	2.354	2.340	113
Reference data from Geller ^a $C_{2h}^3 - C2/m$, monoclinic unit cell		Values calculated from x-ray-diffraction at ambient pressure	
$a_0 = 12.23 \pm 0.02$ Å		$a_0 = 12.188 \pm 0.002$ Å	
$b_0 = 3.04 \pm 0.01$ Å		$b_0 = 3.0389 \pm 0.005$ Å	
$c_0 = 5.80 \pm 0.01$ Å		$c_0 = 5.814 \pm 0.012$ Å	
$\beta = 103.70 \pm 0.02^\circ$		$\beta = 103.78 \pm 0.280^\circ$	

^aReference 23.

The unit-cell volume was determined from the lattice parameters as a function of pressure in the range 0–15 GPa (Fig. 6). It was then fitted to the Birch-Murnaghan equation of state²⁷ (Fig. 6) and yielded a zero-pressure bulk modulus of $K_0 = 191 \pm 4.9$ GPa with $K'_0 = 8.3 \pm 0.9$. If K'_0 is held at 4, the zero-pressure bulk modulus is 208.7 ± 3.6 GPa.

IV. DISCUSSION

All Bragg peaks in the diffraction patterns collected at low pressure (Fig. 3) correspond to the monoclinic β phase of gallium oxide, according to the reference data (CPDS card number 11-370). At the pressures investigated, including ambient, all the observed peaks are broadened. Some of the peaks are not completely resolved, such as the (004) and (10 $\bar{4}$) as well as the (104) and the (11 $\bar{3}$), which correspond to very strong peaks of the β phase. The broadening of the diffraction peaks is assumed to originate basically from the reduced crystallite size and from the broad size distribution. In our composite system, with nanometer-size clusters grown in the surrounding solid medium, the shape distribution, and the surface or interface conditions additionally influence the linewidth, line shape, and relative intensities of the diffraction patterns. A pressure-induced breakdown of peak intensities is especially pronounced in the energy range of 20–30 keV, corresponding to ≈ 2.95 – 2.35 Å. As can be seen from Figs. 3 and 4, with increasing pressure the position of all diffraction peaks systematically shifts towards higher energies and lower d spacings. An increase in pressure to 15 GPa introduces two new diffraction peaks in the energy range of 30–40 keV with interplanar d_{hkl} spacings of ≈ 2.12 and ≈ 1.87 Å. Based on the energy evolution of the Bragg peaks in the diffraction patterns we postulate that a phase transformation occurs in the nanocrystalline phase. Results show that this transition involves a change in the cation coordination number; more specifically this is a transformation from tet-

rahedral to octahedral coordination of the gallium atoms. As pressure rises to 6 GPa, a small intensity shoulderlike feature appears overlapped with the (015) broad peak ($d_{hkl} = 1.85$ Å) of the β phase. When pressure is further increased up to 15 GPa, the peaks assigned to the β phase decrease markedly in intensity and the previously mentioned shoulder is transformed to a well-resolved, broad and intense band of $d_{hkl} = 1.87$ Å (38 keV). At 10 GPa a second new peak appears as a broad, weak intensity band at around 33.5 keV ($d_{hkl} = 2.14$ Å). This band shows a significant, pressure-induced increase in intensity and shifts to $d_{hkl} = 2.12$ Å at 15 GPa. As can be seen from Fig. 3, at 15 GPa the Bragg peak at $d_{hkl} = 2.48$ Å initially assigned to the β phase (111) has a much stronger intensity compared to the peak at 10 GPa. The observed intensity enhancement could be explained by the emergence of a strong peak from the α phase at around 2.47 Å (110) overlapped with (111) of the β phase, according to the reference data (JCPDS card number 43-1013) (Figs. 3 and 4). The overall spectral changes in the energy range of 27–40 keV are explained as due to a phase transition occurring in the gallium oxide nanocrystals. The precise sequence of events during the fourfold to sixfold gallium ions coordination change cannot be specified completely by our studies. However, it appears likely that for such a structural change the phase transition does not occur in a single step. We should rather expect an intermediate buffering phase, most probably emerging at the interface nanocrystal-amorphous matrix, which makes such a change energetically more plausible. The intermediate phase that is supposed to appear between 2 and 6 GPa does not seem to have its own signature except for the pressure-induced intensity evolution at a ≈ 36.5 -keV (≈ 2.0 Å) peak, that starts at 2 GPa and is accompanied at 10 GPa by the development of two new peaks assigned to the α phase.

The three new peaks, starting to emerge between 6 and 10 GPa and well defined at 15 GPa, can therefore be assigned to

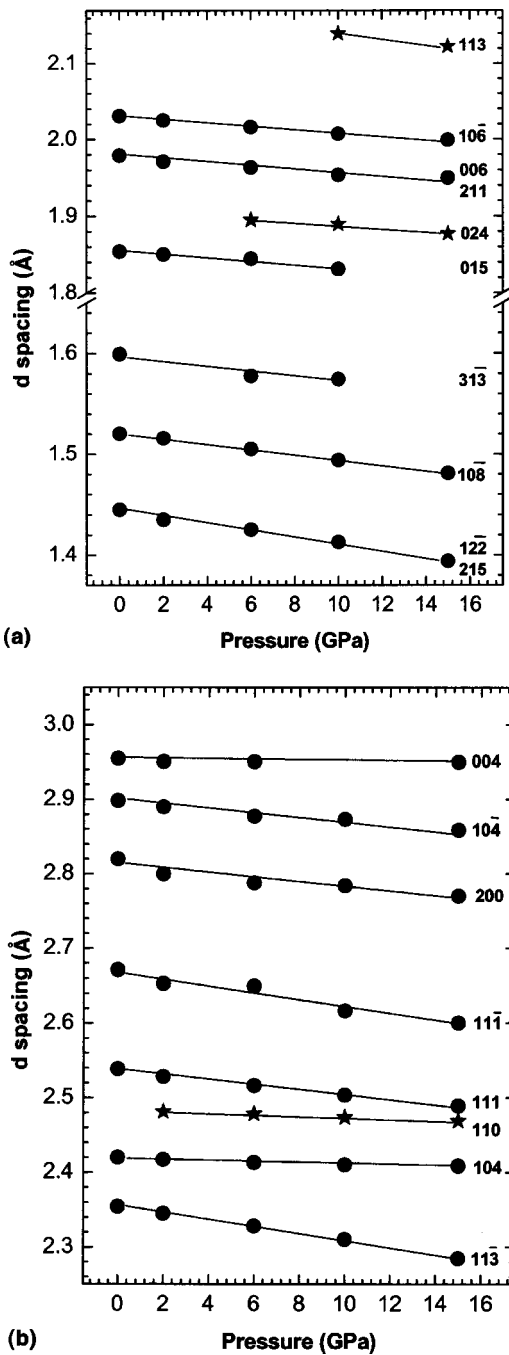


FIG. 4. (a) and (b) Interplanar d_{hkl} spacings of the β - Ga_2O_3 phase as a function of pressure in the range of 0–15 GPa. The solid lines are guides for the eye and emphasize the gradual shift in position of the observed Bragg peaks.

an early stage of a low- (β phase) to high-density (α phase) phase transition of gallium oxide. The obtained results indicate that at 15 GPa the nanocrystalline phase is a combination of β and α phases of gallium oxide. According to the literature, under ambient conditions, the volumes per Ga_2O_3 in the α and β phases are 47.8 and 52.8 \AA^3 , respectively.²³ The crystal structure of β - Ga_2O_3 is monoclinic with unit-cell dimensions $a = 12.23 \pm 0.02$, $b = 3.04 \pm 0.01$, and $c = 5.80 \pm 0.01 \text{ \AA}$, and $\beta = 103.7 \pm 0.3^\circ$ and the crystal belongs

to the space group $C2/m$.^{23,24} The structure has two kinds of coordination for gallium ions, namely, tetrahedral and octahedral with the oxygen ions arranged in a distorted cubic close-packed array. The β - Ga_2O_3 structure appears to be quite different from that of α - Ga_2O_3 , which has the α -corundum structure. The α structure has the oxygen ions in a hexagonal close-packed array with all of the Ga^{3+} ions octahedrally coordinated to oxygen. The existence of the α phase of gallium oxide, reported as metastable at ambient pressure and room temperature, provides evidence that this phase could be stabilized under high-pressure conditions.

Our investigations were focused on the phase transition occurring in a nanocrystalline cluster surrounded by an isotropic amorphous matrix, in the same pressure range for which the literature reports the pressure-induced structural rearrangements of the similar composition host glass matrix. In silica glass the pressure-induced tetrahedral network destabilization includes densification and coordination changes of network-forming units.^{8,14,15,17,28} Contraction of glass under pressure is composed of an elastic part that relaxes immediately after the release of pressure and an inelastic part that brings about the densification.^{8,13,16} While the coordination change is fully reversible (elastic part) some structural modifications in the pressure-quenched sample are consistent with the permanent densification of the glass (inelastic part). Below around 8 GPa, the compression mechanism is thought to be dominated by a decrease in the average value and variation of intertetrahedral angle distribution with negligible tetrahedral distortion, and these changes are reversible on decompression.^{8,11,13–17} Essentially all silicon ions are tetrahedrally coordinated below around 8 GPa but 70% of the silicon ions are octahedrally coordinated and only 3% are tetrahedrally coordinated at 40 GPa.¹⁶ Irreversible changes begin above 8 GPa where silica glass undergoes a gradual increase in the average silicon coordination number from four towards six.^{8,11,13,16,17} These effects are fully consistent with a pressure-dependent shift in ring statistics. This corresponds to a shift in the ring size distribution to smaller ring sizes. The high-pressure structures with average silicon coordination near six have not been quenched to atmospheric pressure (i.e., the increase in coordination is reversed on decompression).^{9,16} However, the decompressed samples are irreversibly densified by up to 20% with the densification due specifically to compressions between 8 and 25 GPa.^{9,12,16,29}

An important question that arises is whether or not one can regard the observed phase transition occurring in the nanocrystalline phase as correlated to the structural transformations occurring in the host silica glass matrix. In the case of uncorrelated gradual transition we can assume that it is based exclusively on inhomogeneous kinetics and interfacial effects. Indeed such gradual transition could result from the nanocrystal size distribution as well as the distribution of interfacial sites and strain energies. The preferred interpretation, however, hints toward the existence of some sort of connection between the structural rearrangements occurring in the host matrix and the phase transition in the nanocrystals. Actually, the instabilities in the tetrahedral network of glass at high pressure, that induce the changes in the silicon

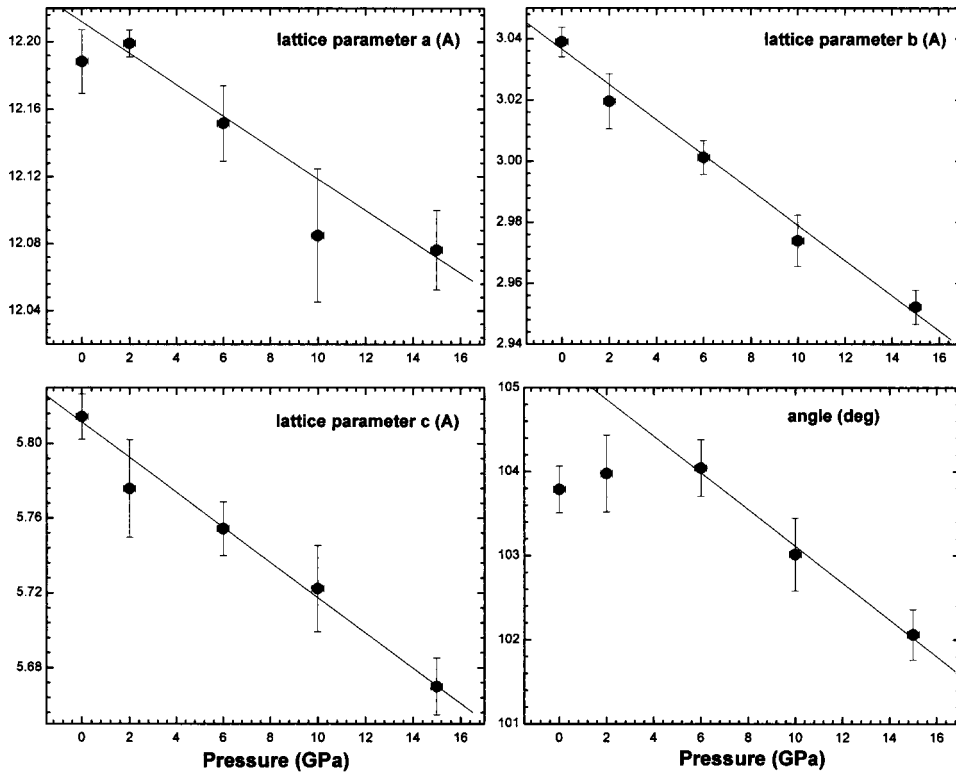


FIG. 5. The unit-cell parameters of the β - Ga_2O_3 phase as a function of pressure. The parameters a , b , and c and the angle β were calculated from the experimental data assuming the monoclinic structure. The solid lines, based on the linear fits, are a guide for the eye and their slopes indicate anisotropy of the unit-cell compressibility.

coordination number and the densification of the amorphous silica network, could trigger the pressure-induced β to α crystalline transition of Ga_2O_3 nanocrystals. However, to shed more light on this possibility further investigations, including vibrational spectroscopy and a comparison with

nanosized granular samples without a host medium, are required.

The stability of a crystallite of a given size is determined by the relative importance of energy per unit volume which favors crystal formation and energy per unit surface area of the opposite sign.^{30–32} Crystallites in the nanosize diameter scale have a large number of atoms within the surface area. Consequently the surface energy contributes substantially to the total energy of the crystallite. It was stated that the phase transition in bulk materials is sharp but for nanocrystals it is broad and occurs at higher pressure.^{33–35} Among the four principal sources that could explain such behavior, including influence of glass matrix, defects, quantum confinement effects, and surface tension, it was found that surface tension is the dominant factor in the phase stability of nanocrystals embedded in a host matrix.^{33,35–37} In addition, studies have shown that stability, hardness, melting point, sintering ability, compressibility, and electronic and magnetic structure are a function of particle diameter. Furthermore, for some materials, there is evidence that the bulk modulus and equation of state also depend on crystallite size.^{36,38,39}

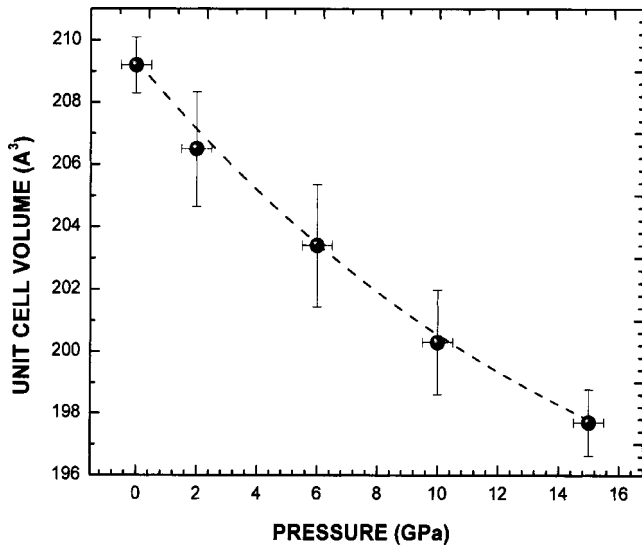


FIG. 6. Evolution of the β - Ga_2O_3 unit-cell volume as a function of pressure. The solid circles represent values calculated from the experimental data under hydrostatic pressure for compression only. The unit-cell volume compression is about 6% compared to ambient conditions. The dashed line is the best fit of Eulerian finite strain (Birch-Murnaghan) equation of state to the experimental data with the bulk modulus $K_0 = 191 \pm 4.9$ GPa, and its pressure derivative $K'_0 = 8.3 \pm 0.9$.

We studied nanocrystals embedded in glass host. What effect does the medium have on the surface or interfacial tension? It was postulated that glasses at high pressure behave as an elastic medium and transmit the pressure to the nanocrystalline phase.³³ In studies of nanometer-size CdS nanocrystals grown by solid-state reaction in a borosilicate glass it was found that they have very low interfacial tension and it was suggested that glass-embedded nanocrystals are inherently quite stable.³⁰ In addition, it was implied that the glass matrix is able to accommodate and relax the strains that might otherwise be found at the surface of the nanoparticles,

increasing their stability.³⁰ These findings are very promising for the potential utility of the composite materials with nanoparticles in glass. To answer all these questions further studies are required, involving composites with various diameters of nanocrystals, a broader pressure range, decompression cycles, and additional experimental techniques.

Figures 5 and 6 show, respectively, how the unit-cell parameters and unit-cell volume both decrease gradually with pressure. Compression increases the field strength exercised on nanoparticles by the surrounding matrix and simultaneously decreases the interplanar d_{hkl} spacings, which correspond to a decrease of Ga-O and Ga-Ga average distance. When pressure is applied (hydrostatic up to about 10 GPa) to the composite material, the volume of nanocrystalline clusters decreases, which results in a decrease in the unit-cell volume calculated to be 6%, between ambient and 15 GPa, indicating a progressive densification of the nanocrystalline phase.

To analyze the pressure-volume (P - V) data we applied the Birch-Murnaghan equation of state.²⁷ This Eulerian finite strain formalism is based on the assumption that the strain energy of a solid undergoing compression can be expressed as a Taylor series in the finite strain:

$$P = 3K_0 f_v (1 + 2f_v)^{5/2} [1 + a f_v + b f_v^2 + \dots],$$

where K_0 is the bulk modulus, $a = 3(K'_0 - 4)/2$ is the third-order coefficient, $f_v = 0.5 * [(V_0/V)^{2/3} - 1]$ is the Eulerian strain, and V_0 and V are the elementary unit volume at zero and at a given pressure, respectively.

Defining the normalized pressure as $F_v = P[3f_v(1 + 2f_v)^{2.5}]^{-1}$ yields the second-order finite strain equation

$$F_v = K_0 [1 - 1.5(4 - K'_0)f_v].$$

Since K'_0 is close to 4 for most materials, we used the second-order equation of state to estimate the zero-pressure bulk modulus $K_0 = 209 \pm 3.6$ GPa. By fitting the P - V data in the form of F - f (third-order equation of state), we estimated $K_0 = 191 \pm 4.9$ and $K'_0 = 8.3 \pm 0.9$ GPa from the intercept and the slope, respectively.

V. CONCLUSION

The subject of our work was to use high pressure to alter systematically the local structure of nanosized aggregates dispersed in an amorphous matrix. We applied a synchrotron-

radiation-based x-ray-diffraction technique and a diamond-anvil cell to follow *in situ* the pressure-induced alterations in the ligand field experienced by gallium oxide nanocrystals embedded in a silicon oxide-based glass matrix. The focus was to elucidate how elevated pressure modifies the gallium oxide nanocrystals' structure, stimulating transitions from low- to high-density phases. Distinctive changes in the energy-dispersive x-ray-diffraction patterns have been analyzed in light of a phase transition occurring in the nanocrystalline phase, beginning at around 6 GPa. Results revealed that this phase transition involves a change in the coordination number of metal cations and produces a transformation from a low- to a high-density phase. The overall modification of x-ray-diffraction patterns demonstrated a pressure-induced β -Ga₂O₃ to α -Ga₂O₃ phase transition occurring in the nanocrystalline phase. The obtained results indicate that at 15 GPa the nanocrystalline phase is a combination of β and α phases of gallium oxide. We hypothesize that the beginning of the pressure-induced coordination change and densification occurring in the glass matrix surrounding the nanocrystal could be correlated to the phase transition detected in the nanocrystalline phase. This phase transition is sluggish and is not completed by 15 GPa, where the dominant crystalline phase is still β -Ga₂O₃. It is reasonable to expect that for some pressure beyond 15 GPa, with further densification of the nanocrystalline phase, the α phase, being denser than β , will be more pronounced. To shed more light on our hypothesis further studies are required, involving composites with various diameters of nanocrystals, a broader pressure range, decompression cycles, and additional experimental techniques.

ACKNOWLEDGMENTS

This work was supported by the National Science Foundation (U.S.) and the Advanced Research Institute for Science and Engineering, Waseda University, Tokyo (Japan). The authors acknowledge the Nippon Electric Glass Company, Kyoto (Japan), and especially Dr. A. Sakamoto, for technical advice and the use of their facilities for sample preparation. We thank also Dr. L. Binet from l'Ecole Normale Supérieure de Chimie de Paris (France) for sending us the reference x-ray-diffraction data of different gallium oxide structures. The X17C of NSLS is supported by NSF and DOE-NSLS grants.

*Corresponding author. Present address: Department of Chemistry, University of Wyoming, Laramie, WY 82071. Email address: crystapost@hotmail.com

†Present address: University of Central Florida, CREOL, Department of Physics, Orlando, FL.

¹R. Ceccato, R. Dalmaschio, A. Gialanella, G. Mariotto, M. Montagna, F. Rossi, M. Ferrari, K. E. Lipinska-Kalita, and Y. Ohki, *J. Appl. Phys.* **90**, 2522 (2001).

²A. Stepanov, D. E. Hole, and P. D. Townsend, *J. Non-Cryst. Solids* **260**, 65 (1999).

³G. DeMarchi, F. Gonella, and P. Mazzoldi, *J. Non-Cryst. Solids*

196, 79 (1996).

⁴S. J. L. Ribeiro, P. Dugat, D. Avignant, and J. Dexpert-Ghys, *J. Non-Cryst. Solids* **197**, 8 (1996).

⁵F. Auzel, K. E. Lipinska-Kalita, and P. Santa-Cruz, *Opt. Mater. (Amsterdam, Neth.)* **5**, 75 (1996).

⁶K. E. Lipinska-Kalita, G. Mariotto, and F. Zanghellini, *Philos. Mag. B* **71**, 547 (1995).

⁷C. Strohhoefer, J. Fick, H. C. Vasconcelos, and R. M. Almeida, *J. Non-Cryst. Solids* **226**, 182 (1998).

⁸C. Meade, R. J. Hemley, and H. K. Mao, *Phys. Rev. Lett.* **69**, 1387 (1992).

- ⁹C. S. Zha, R. J. Hemley, H. K. Mao, T. S. Duffy, and C. Meade, *Phys. Rev. B* **50**, 13 105 (1994).
- ¹⁰A. Doi, *Phys. Rev. B* **63**, 184202 (2001).
- ¹¹M. M. Roberts, J. R. Wienhoff, K. Grant, and D. J. Lacks, *J. Non-Cryst. Solids* **281**, 205 (2001).
- ¹²M. Grimsditch, *Phys. Rev. Lett.* **52**, 2379 (1984).
- ¹³S. O. E. Nosakhareorodeoremwanta and D. J. Lacks, *Phys. Rev. B* **66**, 212101 (2002).
- ¹⁴H. Sugiura and T. Yamadaya, *J. Non-Cryst. Solids* **144**, 151 (1992).
- ¹⁵C. H. Polsky, K. H. Smith, and G. H. Wolf, *J. Non-Cryst. Solids* **248**, 159 (1999).
- ¹⁶D. J. Lacks, *Phys. Rev. Lett.* **80**, 5385 (1998).
- ¹⁷R. J. Hemley, H. K. Mao, P. M. Bell, and B. O. Mysen, *Phys. Rev. Lett.* **57**, 747 (1986).
- ¹⁸R. Ceccato, R. Dalmaschio, M. Ferrari, K. E. Lipinska-Kalita, G. Mariotto, M. Montagna, and Y. Ohki, *J. Raman Spectrosc.* **32**, 643 (2001).
- ¹⁹L. Binet and D. Gourier, *Appl. Phys. Lett.* **7**, 1138 (2000).
- ²⁰Z. Hajnal, J. Miro, G. Kiss, F. Reti, P. Deak, C. Herndon, and J. M. Kuperberg, *J. Appl. Phys.* **86**, 3792 (1999).
- ²¹N. Ueda, H. Hosono, R. Waseda, and H. Kawazoe, *Appl. Phys. Lett.* **70**, 3561 (1997).
- ²²M. Passlack, E. F. Schubert, W. S. Hobson, M. Hong, N. Moriya, S. N. G. Chu, K. Constadinidis, J. P. Mannaerts, M. L. Schnoes, and G. J. Zydzik, *J. Appl. Phys.* **77**, 686 (1995).
- ²³S. Geller, *J. Chem. Phys.* **33**, 676 (1966).
- ²⁴J. Ahmen, G. Svensson, and J. Albertson, *Acta Crystallogr., Sect. C: Cryst. Struct. Commun.* **C52**, 1336 (1996).
- ²⁵D. E. Warren, *X-Ray Diffraction* (Dover, New York, 1990).
- ²⁶D. L. Heinz and R. Jeanloz, *J. Appl. Phys.* **55**, 885 (1984).
- ²⁷F. Birch, *J. Geophys. Res. B* **83**, 1257 (1978).
- ²⁸P. J. Itie, A. Polian, G. Calas, J. Petiau, A. Fontaine, and H. Tolentino, *Phys. Rev. Lett.* **63**, 398 (1989).
- ²⁹A. Polian and M. Grimsditch, *Phys. Rev. B* **41**, 6086 (1990).
- ³⁰T. M. Hayes, L. B. Lurio, J. Pant, and P. D. Persans, *Phys. Rev. B* **63**, 155417 (2001).
- ³¹P. D. Persans, L. B. Lurio, J. Pant, H. Yukselici, G. Lian, and T. M. Hayes, *J. Appl. Phys.* **87**, 3850 (2000).
- ³²H. Yukselici, P. D. Persans, and T. Hayes, *Phys. Rev. B* **52**, 11 763 (1995).
- ³³M. R. Silvestri and J. Schroeder, *J. Phys.: Condens. Matter* **7**, 8519 (1995).
- ³⁴X. S. Zhao, J. Schroeder, P. D. Persans, and G. Bilodeau, *Phys. Rev. B* **43**, 12 580 (1991).
- ³⁵C. C. Chen, A. B. Herhold, C. S. Johnson, and A. P. Alivisatos, *Science* **276**, 398 (1997).
- ³⁶S. H. Tolbert, A. B. Herhold, L. E. Brus, and A. P. Alivisatos, *Phys. Rev. Lett.* **76**, 4384 (1996).
- ³⁷J. N. Wickham, A. B. Herhold, and A. P. Alivisatos, *Phys. Rev. Lett.* **84**, 923 (2000).
- ³⁸S. H. Tolbert, A. B. Herhold, C. S. Johnson, and A. P. Alivisatos, *Phys. Rev. Lett.* **73**, 3266 (1994).
- ³⁹S. H. Tolbert and A. P. Alivisatos, *J. Chem. Phys.* **102**, 4642 (1995).